

Pollen dispensing schedules in buzz-pollinated plants: Experimental
comparison of species with contrasting floral morphologies

Jurene E. Kemp^{1,*}

Mario Vallejo-Marín¹

¹Department of Biological and Environmental Sciences, University of Stirling. Stirling, Scotland,
United Kingdom, FK9 4LA.

*Author for correspondence:

Email: jurenekemp@yahoo.com

Manuscript received _____; revision accepted _____.

Running title: Pollen dispensing schedules in buzz-pollinated plants

This is the peer reviewed version of the following article: Kemp, J. E., and Vallejo-Marín, M.. 2021. Pollen dispensing schedules in buzz-pollinated plants: experimental comparison of species with contrasting floral morphologies. *American Journal of Botany* 108(6): 993– 1005, which has been published in final form at <https://doi.org/10.1002/ajb2.1680>. This article may be used for non-commercial purposes in accordance with Wiley Terms and Conditions for self-archiving.

ABSTRACT

Premise: Plants can mitigate the fitness costs associated with pollen consumption by floral visitors by optimizing pollen release rates. In buzz-pollinated plants, bees apply vibrations to remove pollen from anthers with small pores. These poricidal anthers potentially function as mechanism staggering pollen release, but this has rarely been tested across plant species differing in anther morphology.

Methods: In *Solanum* section *Androceras*, three pairs of buzz-pollinated species have undergone independent evolutionary shifts between large- and small-flowers, which are accompanied by replicate changes in anther morphology. We used these shifts in anther morphology to characterise the association between anther morphology and pollen dispensing schedules. We applied simulated bee-like vibrations to anthers to elicit pollen release, and compared pollen dispensing schedules across anther morphologies. We also investigated how vibration velocity affects pollen release.

Key Results: Replicate transitions in *Solanum* anther morphology are associated with consistent changes in pollen dispensing schedules. We found that small-flowered taxa release their pollen at higher rates than their large-flowered counterparts. Higher vibration velocities resulted in quicker pollen dispensing and more total pollen released. Finally, both the pollen dispensing rate and the amount of pollen released in the first vibration were negatively related to anther wall area, but we did not observe any association between pore size and pollen dispensing.

Conclusions: Our results provide the first empirical demonstration that the pollen dispensing properties of poricidal anthers depend on both floral characteristics and bee vibration properties. Morphological modification of anthers could thus provide a mechanism to exploit different pollination environments.

Key words: buzz pollination, biomechanics, pollen presentation theory, poricidal anther morphology, *Solanum*, sonication.

INTRODUCTION

Most flowering plant species rely on animals to transport pollen between conspecific flowers for fertilisation (Ollerton et al., 2011). Despite the widespread reliance on animals as pollen vectors, animal pollination can limit pollen dispersal, particularly when visitors actively collect pollen, making it unavailable for fertilisation (Harder and Wilson, 1994; Minnaar et al., 2019). In nectarless plants, where pollen serves both pollinator reward and vehicles for male gametes, we expect selection to favour adaptations that limit the fitness costs associated with pollen consumption, whilst releasing enough pollen to ensure sufficient pollinator visits (Harder and Thomson, 1989; Harder and Barclay, 1994; LeBuhn and Holsinger, 1998; Vallejo-Marín et al., 2009). Plants can theoretically mitigate the fitness costs associated with pollen consumption by optimizing their pollen dispensing schedules (i.e., the rate at which pollen is released across visits) to the visitation rates and grooming behaviours of pollinators (Harder and Thomson, 1989; Harder and Wilson, 1994; LeBuhn and Holsinger, 1998).

Theoretical models predict that pollen should be gradually released across multiple visits when pollinator visits are unlimited and when their grooming behaviours result in high diminishing fitness returns (i.e., when the total amount of pollen transferred decreases with the amount of pollen collected per visit) (Harder and Thomson, 1989; Harder and Wilson, 1994). In contrast, when pollinator visits are limited and have high per-visit transfer efficiencies, pollen should be released across fewer visits (Harder and Thomson, 1989; Harder and Wilson, 1994). Thus, when pollinators collect pollen and exhibit low per-visit transfer efficiencies, as in many bee pollinated taxa, models predict that selection will favour pollen being gradually released across multiple visits if pollinators are abundant (Thomson, 1986; Harder and Thomson, 1989; Holsinger and Thomson, 1994; Schlindwein et al., 2005; Harder and Johnson, 2009). However, restricting pollen removal excessively might be in conflict with the requirements of pollinators that collect pollen, and pollinators might avoid visiting flowers that release too little pollen per visit (Harder, 1990). Pollen dispensing schedules thus represent the evolutionary outcome of selective pressures acting on plants and mediated by pollinators, and are particularly important in plants that offer pollen as the primary reward (Harder and Barclay, 1994).

Plants can dispense pollen gradually through moderating anther maturation within a flower or by staggering flower opening within a plant individual (Sargent, 2003; Castellanos et al., 2006a; Li et al., 2014). Another potential solution to limit per-visit pollen collection is to physically restrict access to pollen, as is done in poricidal anthers that contain pollen inside the anthers (Buchmann et al., 1977; Harder and Barclay, 1994; Dellinger, Pöllabauer, et al., 2019). Poricidal anthers are associated

with buzz-pollination (Buchmann, 1983). During buzz pollination, bees vibrate flowers using their thoracic muscles. The vibrations transmitted through the anthers cause pollen to be ejected through the apical pores (De Luca and Vallejo-Marín, 2013; Vallejo-Marín, 2019). Buzz-pollinated flowers are typically nectarless and solely offer pollen as reward (Buchmann, 1983; Faegri, 1986; Vallejo-Marín et al., 2010), which makes them a likely candidate for gradual pollen release. Buzz-pollination is widespread among plants, with more than 20,000 species possessing poricidal anthers (Buchmann, 1983), and about half of bee species capable of producing floral vibrations (Buchmann, 1983; Cardinal et al., 2018). The floral and anther morphology of buzz-pollinated flowers is very diverse, and even plants with poricidal anthers vary widely in their stamen morphology, both between and within species (Buchmann, 1983; Dulberger et al., 1994; Corbet and Huang, 2014; Vallejo-Marín et al., 2014; Dellinger, Artuso, et al., 2019; Dellinger, Chartier, et al., 2019). Similarly, the vibration properties of bees vary across and within species (King and Buchmann, 2003; Arceo-Gómez et al., 2011; Corbet and Huang, 2014; Arroyo-Correa et al., 2019; De Luca et al., 2019; Pritchard and Vallejo-Marín, 2020), and previous empirical work demonstrates that vibration properties, particularly their amplitude, affect pollen release (Harder and Barclay, 1994; King and Buchmann, 1996; De Luca et al. 2013). However, we know relatively little about how plant species with different anther and floral morphologies vary in their pollen release schedules (but see Harder and Barclay 1994, Dellinger et al. 2019), including their response to vibrations of different amplitudes.

Anther properties, such as shape, length, natural frequency and pore size, are theoretically expected to influence pollen release (Buchmann and Hurley, 1978; Vallejo-Marín et al., 2009). In what remains the only biophysical model of buzz pollination, Buchmann and Hurley (1978), modelled a poricidal anther with a simple geometry (a rectangular box) and an anther pore at one end. The anther vibrates along a single spatial axis perpendicular to the longest anther dimension, with pollen grains bouncing against the interior walls of the anther locule. In this model, pollen release occurs when the kinetic energy of the vibrating anthers is transferred to the pollen grains, which are then ejected through the pore. The higher the energy, the higher the pollen release rate. Pollen grains can gain energy as they bounce against the interior of the anther walls or against each other. Thus, the internal surface area of the anther locule along the axis of vibration (A) is positively related with the rate of change in energy of pollen grains (equation 9 in Buchman and Hurley, 1978). However, energy can also be lost as pollen grains escape the anther through the pore, and therefore the area of the anther pore (A') is negatively related to changes in pollen energy (eqn. 9). Because A' is positively related to the rate at which pollen grains are released from anthers (equation 10), but negatively related to changes in pollen's kinetic energy, the relationship between anther pore size and pollen release dynamics is not immediately obvious, as dynamics change as the anther empties

while vibrated. Numerical integration of Buchman and Hurley's model suggests that both increased anther wall area and pore size should result in faster times to empty anthers, and larger anther volumes should result in slower pollen release (B. Travacca and M. Vallejo-Marín, unpublished), but clearly more theoretical work is needed in this area.

In contrast to the absence of work on associations between anther morphology and pollen release rates, the effect of the type of vibration applied (e.g., vibration frequency, amplitude and duration) on pollen release has received more attention (Harder and Barclay, 1994; De Luca et al., 2013; Rosi-Denadai et al., 2018). A study using bee-like vibrations (in terms of frequency, duration and amplitude) showed that pollen release is more strongly affected by amplitude and duration than by the frequency of the vibration (De Luca et al., 2013). However, previous studies assessing the effects of vibration properties on pollen release have focused on the amount of pollen released during a single vibration, and thus it has not been possible to build a full picture of pollen release curves following multiple consecutive buzzes.

Here, we characterise pollen dispensing schedules across three pairs of closely related buzz-pollinated taxa in the genus *Solanum* section *Androceras* (Solanaceae). These six taxa represent three pairs of independent evolutionary transitions from large flowers with large anthers and small pores, to small flowers with small anthers and large pores (Whalen 1978; 1979; Vallejo-Marín et al., 2014; Rubini-Pisano et al., in prep). These large- to small-flower transitions bear the classic hallmark traits of shifts in mating system from outcrossing towards increased self-pollination (Vallejo-Marín et al., 2014; Rubini-Pisano et al., in prep), but have also been suggested to be associated with pollinator shifts (Whalen, 1978). Regardless of the cause of the shift in flower and anther morphology, these changes allow us to investigate the association between anther morphology and pollen dispensing schedules in closely related taxa. We first investigate whether these replicate transitions in general floral morphology are associated with replicate changes in pollen dispensing schedules. We then use one of these evolutionary transitions from large- to small-flowered species to investigate the extent to which pollen dispensing schedules depend on vibration velocity. Finally, we test whether the parameters in the Buchmann and Hurley (1978) model can predict pollen release rates in the six focal taxa. The replicate evolutionary transitions in anther morphology in three closely related clades of *Solanum* provide an ideal opportunity to establish how pollen dispensing schedules of buzz-pollinated plants vary with anther morphology, and how this is influenced by vibration properties.

MATERIALS AND METHODS

Study system-

Solanum (Solanaceae) is often used as a model system for studying buzz-pollination (Vallejo-Marín 2019). This genus contains c. 1,350 species with nectarless flowers, representing about half of the species diversity in the family Solanaceae (Särkinen et al., 2013). *Solanum* flowers are pentamerous, usually radially symmetric, and bear poricidal anthers (Harris, 1905; Knapp, 2002). During buzz-pollination, bees typically grab the base of the anthers using their mandibles whilst curling the ventral side of their bodies around the anthers. They then use their indirect flight muscles to vibrate the anthers to instigate pollen release (King et al., 1996). *Solanum* section *Androceras* is a monophyletic clade consisting of approximately 12 annual and perennial species distributed in Mexico and the southern USA (Whalen, 1978; Stern et al., 2010). All taxa in section *Androceras* are heterantherous, i.e., have two or more morphologically differentiated sets of anthers in the same flower. In heterantherous species, one set of anthers is usually associated with pollinator attraction and reward (“feeding” anthers), while the other set contributes disproportionately to fertilising ovules (“pollinating” anthers) (Vallejo-Marín et al., 2009). The section is divided into three series: *Androceras*, *Pacificum*, and *Violaceiflorum* (Whalen, 1979). Parallel shifts in flower and anther morphology have occurred within each of these three series (Vallejo-Marín et al., 2014) (Figs. 1 & 2). In series *Androceras*, *S. rostratum* has large flowers, and long anthers with small anther pores, whereas *S. fructu-tecto* has small flowers with small anthers and large anther pores (referred to as the SR-SF clade, hereafter). Similar morphological shifts are present in series *Pacificum* for *S. grayi* var. *grandiflorum* (large flowers) and *S. grayi* var. *grayi* (small flowers) (referred to as the SGN-SGG clade, hereafter), and in series *Violaceiflorum* for *S. citrullifolium* (large flowers) and *S. heterodoxum* (small flowers) (referred to as the SC-SH clade hereafter). These shifts in floral morphology is potentially associated with shifts in mating system (i.e., from outcrossing to selfing), although this has not been empirically confirmed (Vallejo-Marín et al., 2014). Within these species pairs, the pollinating and feeding anthers are less differentiated in the small flower types than in the large flower types (Vallejo-Marín et al., 2014). We refer to these two distinct floral morphologies as the ‘small flower type’ and ‘large flower type’ throughout.

Seed collection and plant growth-

Seeds were collected from natural populations in Mexico between 2007 and 2010, except for *S. citrullifolium* which was obtained from the Solanaceae collection at Radboud University, Netherlands (Experimental Garden and Genebank Solanaceae collection). For each plant species, we used seeds from a single population. Accession numbers and sample localities are provided in Appendix S1 (see Supplemental Data with this article). Germination was induced by treating seeds for 24h with 1000 ppm aqueous solution of gibberellic acid (GA3; Sigma-Aldrich, Dorset, UK), following the method of Vallejo-Marín et al. (2014). Two to four weeks after germination, seedlings were transplanted to 1.5

L pots and kept in a pollinator-proof greenhouse with natural light supplemented with compact fluorescent lamps to provide at least 16 hours of daylight. Supplemental heating was provided to maintain minimum temperatures above 16°C (night) and 25°C (day).

Synthesising bee-like vibrations and playback system-

To characterise pollen dispensing schedules, we applied mechanical vibrations to flowers. We used Audacity v2.1.3 (<http://audacity.sourceforge.net/>) to generate an artificial vibration (stimulus) with similar frequency properties to the vibrations that bees produce when extracting pollen (De Luca and Vallejo-Marín, 2013). The vibrations consisted of a pure tone (300 Hz) sine wave made of five consecutive pulses of 200 milliseconds (ms) each with 200 ms of silence between pulses (i.e., total stimulus length = 2 seconds). Each pulse had a fade-in feature of 10 ms (Appendix S2). Multiple short buzzes with a single dominant frequency characterise the floral vibrations of buzz pollinating bees (De Luca and Vallejo-Marín, 2013, Pritchard and Vallejo-Marín, 2020), and a 300 Hz frequency was selected to capture the frequency of floral vibrations typically produced by medium-sized bees, including bumblebees (De Luca and Vallejo-Marín, 2013; Switzer and Combes, 2017; Arroyo-Correa et al., 2019; De Luca et al., 2019; Pritchard and Vallejo-Marín, 2020). Previous studies have shown that variation in frequency does not alter pollen release in a single vibration, but rather, higher accelerations result in higher pollen release (De Luca et al., 2013). Theoretically, if flowers are vibrated at the natural frequency of anthers, higher pollen release could be induced due to the higher accelerations associated with resonance (King and Buchmann, 1996). For our six taxa, Nunes (2020) showed that only the feeding anthers of *S. grayi grayi* might resonate at 300 Hz (mean natural frequency = 294 Hz). We thus used a single ecologically relevant frequency for all experiments (i.e. 300 Hz), and we vary acceleration in the experiments (described below). The vibration amplitude was calibrated as described below to obtain the appropriate velocity for each experiment.

The synthesised vibrations were applied using a custom-made vibration transducer system (A. Gordon and M. Vallejo-Marín, unpublished; Appendix S3). This playback system consisted of a vibration transducer speaker (Adin S8BT 26W, Shenzhen, China) with a vibrating metal plate. We attached a metal rod (15 cm long with a 0.5 cm diameter) using an ethyl cyanoacrylate glue (Loctite UltraGel Control, Düsseldorf, Germany) and plastic supports at the base. We fixed a pair of featherlight forceps (D4045, Watkins & Doncaster, Leominster, UK) to the distal end of the metal rod at a 90° angle using a metal clip. We used laser vibrometry to calibrate the vibration amplitude and check that the playback frequency matched the input frequency. Briefly, we deployed a PDV-100 laser vibrometer (PDV-100, Polytec, Waldbronn, Germany) and focused the laser close to the tip of

the forceps (~1 cm from the tip), where we had placed a small amount of reflective tape. The laser beam was aimed on the forceps perpendicular to the main axis of displacement of the transduction system. The vibration signal was played in Audacity using a laptop computer connected to the transduction system. The frequency and amplitude of the vibration was checked using VibSoft-20 data acquisition and software (Polytec, Waldbronn, Germany). Peak amplitude velocity of the vibration was adjusted using the volume control in the computer until the desired velocity was obtained. This calibration was done at the beginning of every day of the experiment, and again after pollen was extracted from 3-5 flowers.

Pollen extraction and counting-

Experimental flowers were brought from the glasshouse between 7h00 and 9h00 on the first day of flower opening in a closed container with wet floral foam (Oasis Floral Products, Washington, UK), to prevent flowers from drying out. Closed flower buds were tagged on the previous day in the late afternoon to ensure that only newly opened flowers are used in the experiments. All pollen extraction treatments were done within three hours after the flowers were picked. Maximum ten flowers were used per day, depending on availability, and multiple plant species were used each day. The artificial stimuli were applied to flowers in May 2019 at room temperature (22°C) in an indoor airconditioned laboratory at the University of Stirling.

An individual flower, including the pedicel, was attached to the vibration transducer system using the forceps. The forceps were used to hold the flower at the base of the five anthers (cf. De Luca et al., 2013), and vibrations were thus directly transferred to the anthers in a similar manner as when bees vibrate flowers. A single vibration (consisting of five 200 ms buzzes as described above), was applied to the anthers of a flower, and the ejected pollen was collected in a 1.5 mL microcentrifuge vial. Each flower was subjected to 30 consecutive vibrations for a grand total of 30 s of buzzing time. Pollen was collected in separate vials for vibrations 1—10, 15, 20, 25, and 30. At the end of the trial, we removed the anthers of the flower and placed them in a centrifuge tube with 200 µl of 70% ethanol. Each trial lasted 10-15 minutes. The remaining pollen in the flower was extracted later with the help of a sonicating bath (D00351, Premier Farnell Ltd., Leeds, UK), which allowed us to calculate the total amount of pollen grains in each flower we used in our pollen dispensing trials.

To estimate the number of pollen grains in each sample (including samples of the pollen remaining in anthers), we used a particle counter (Multisizer 4e Coulter Counter, Indianapolis, USA). Each pollen sample (suspended in 200 µl 70% ethanol) was added to 20 mL 0.9% NaCl solution. For each sample, the amount of pollen was counted in two 1 mL subsamples. The pollen counts for these subsamples were averaged and multiplied by 20 to obtain the total pollen count. For samples

with higher pollen concentrations, such as those containing the pollen remaining in the anther, we added the pollen samples to 100 or 200 mL NaCl solution and multiplied the averaged pollen count by 100 or 200 respectively to obtain the total pollen count. Blank samples, containing only 0.9% NaCl solution were run at the beginning of a session and regularly between samples to ensure calibration accuracy.

Characterising pollen dispensing curves-

To characterize the pollen dispensing curves, we fitted exponential decay curves for each flower using the *nls* function in R ver. 3.6.0 (R Core Team, 2019). The decay curves followed the function:

$$y = a * (1 - b)^x$$

where *y* represents the percentage of pollen released in a vibration, and *x* represents the vibration number. The parameter *a* represents the intercept of the pollen dispensing curve, and the parameter *b* represents the percentage decrease in the amount of pollen released in each successive vibration (e.g., if *b* = 0.3, then 30% of the remaining pollen is released in each successive vibration). Model parameters were estimated separately for each flower using the *nls* function. The percentage pollen released per vibration was calculated by dividing the amount of pollen released per vibration by the total amount of pollen in a flower.

Measuring anther traits-

For each flower used in our trials, we measured three traits for the pollinating and feeding anthers separately, after pollen had been extracted. We measured: (1) the anther length, (2) the anther breadth at base of the anther, and (3) the area of the pores (Appendix S4). Anther length and breadth were measured using a dissection microscope and callipers. For each flower, all four feeding anthers were measured, and lengths and breadths were averaged across the feeding anthers to calculate a single value per flower. To calculate the anther pore area, we took SEM photographs of one feeding and one pollinating anther per flower, and we measured the area of the pores from photographs using ImageJ v1.52 (Schneider et al., 2012). Variation in traits between species can be seen in Figs. 1 & 2.

Variation in pollen dispensing curves across flower types-

To assess whether pollen dispensing schedules vary between flower types, we subjected *Solanum rostratum*, *S. fructu-tecto*, *S. grayi* var. *grandiflorum*, *S. grayi* var. *grayi*, *S. citrullifolium*, and *S. heterodoxum* flowers to simulated vibration stimuli as described above. All vibration stimuli had a peak velocity of 80 mm/s. We used this velocity as it corresponds to velocities which have been

recorded for bees on flowers (De Luca and Vallejo-Marín, 2013). Pollen dispensing curves were characterized for ten flowers per species, except for *S. fructu-tecto* where only five flowers were used.

To compare the pollen dispensing curves, we extracted two response variables from each curve. Firstly, we extracted the amount of pollen released from the first simulated vibration, which reflects the amount of pollen reward a pollinator will receive in a single visit. Secondly, we estimated the rate of pollen release (i.e., the dispensing rate) as represented by b in the exponential decay function. For example, if $b = 0.2$, then 20% of the remaining pollen in the anther is released in each sequential vibration.

To compare pollen dispensing between small and large flower types, we analysed each of the three phylogenetic pairs separately (series *Androceras*, *Pacificum* and *Violaceiflorum*). After testing for normality, we used nonparametric Wilcoxon rank sum tests. We chose to perform three separate within-clade tests, instead of a single parametric omnibus test across all species, because both the non-normality of our data and our small sample sizes that would prevent fitting more complex parametric models with clade * anther-type interactions. Importantly, our tests allow assessing whether differences between small- and large-flowered species are clade specific. Because we performed multiple tests, we used the Holm method to adjust p-values (similar to the Bonferroni correction but with a lower risk of introducing type II error). In addition to releasing pollen across multiple vibrations, plants can potentially further stagger pollen release across hours or days. We tested for this by comparing the total percentage of pollen that was released from anthers across the 30 vibrations between anther types within clades using Wilcoxon rank sum tests with Holm-adjusted p-values.

Effect of vibration properties on pollen dispensing-

We assessed the influence of vibration properties on pollen dispensing schedules by applying simulated vibrations to flowers of two species: *Solanum citrullifolium* (large flower type) and *S. heterodoxum* (small flower type). We focused on the effects of variation in velocity because previous work has shown that velocity is positively associated with the amount of pollen released in a single vibration (De Luca et al., 2013). We applied three peak velocity treatments: 80, 40, and 20 mm/s. These values are within the range of previously recorded bee vibrations (De Luca et al., 2013). Dispensing curves were characterized for nine to ten flowers for each treatment and species (Table 1). We used the same response variables as in the previous section (i.e., percentage of pollen released in the first vibration and the dispensing rate), and we compared these response variables across the three velocity treatments within each species separately using analysis of variance

(ANOVA) and Tukey posthoc tests. Further, we compared the total amount of pollen released per treatment within each species using ANOVA and Tukey posthoc tests.

Association between pollen dispensing schedules and anther traits-

If consistent differences are found between large- and small-flowered taxa, the question of what causes those differences remains. One hypothesis is that the anther traits specified in the Buchmann and Hurley (1978) model predicts the rate of pollen release. The anther traits Buchmann and Hurley (1978) used in their model of pollen release from poricidal anthers include the area of the pore (A'), the area of the anther locule along the wall perpendicular to the movement direction of the anther (A), and the internal volume of the anther's locule (ϑ). Because of the complexity of anther shapes and the technical difficulty of accurately estimating the internal dimensions of the anther locule, we used external anther area (length x breadth of the anther; Buchmann and Hurley, 1978; Appendix S4) as a proxy of locule area A . We kept the pollinating and feeding anther traits separately, rather than combining their areas, because of the morphological differences between these anther types which may have different effects on pollen release. Further, because flowers contain four feeding anthers and one pollinating anther, we multiplied the values of both the pore area and the anther wall area of the feeding anther by four to obtain total areas for each flower. Because kinetic energy was kept constant in our pollen extraction trials, we could directly assess the association between pollen dispensing schedules and anther traits.

To determine whether the amount of pollen released in the first vibration is related to anther traits, we implemented a negative binomial mixed effect model (LMM) in *lme4* (Bates et al., 2015). We used the amount of pollen released in the first vibration as response variable and the four anther traits (i.e., pore area and anther wall area for pollinating and feeding anthers separately) as predictor variables. Because the total amount of pollen grains varied between flowers, we also included the total amount of pollen grains per flower as offset in the model. We added species identity as a random effect. Similarly, we evaluated the association between pollen dispensing rate and anther traits. Because the dispensing rate metric (b) is bounded between 0 and 1, we conducted a logistic mixed effect model (GLMM) using the dispensing rate as the response variable and the four anther traits as the predictor variables, with species identity as a random effect.

RESULTS

Pollen dispensing-

Plant species varied in the amount of pollen grains that were present in flowers, with *Solanum heterodoxum* containing the fewest pollen grains ($22 \times 10^3 \pm 8 \times 10^3$; median \pm se) and *S. grayi* var. *grandiflorum* containing the most ($446 \times 10^3 \pm 17 \times 10^3$; Table 1). Small-flowered taxa consistently contained fewer pollen grains than their large-flowered counterparts (Table 1). The amount of pollen released decreased gradually with an increasing number of vibrations applied, and no pollen was released by the 30th vibration (Fig. 3), despite large amounts of pollen remaining in the anthers (Fig. 4c). The pollen dispensing curves thus showed exponential decay, with most pollen released in the first vibration (Fig. 3).

Variation in pollen dispensing schedules between flower types-

The percentage of pollen released in the first vibration varied between flower types, and for all three phylogenetic clades, more pollen was released in the first vibration for small flower types than large flower types (SC-SH: $W = 8$, $p < 0.001$, $p_{\text{adjusted}} = 0.002$; SR-SF: $W = 1$, $p = 0.001$, $p_{\text{adjusted}} = 0.003$; SGN-SGG: $W = 18$, $p = 0.01$, $p_{\text{adjusted}} = 0.01$; Table 1; Figs. 3 & 4). Across our six taxa, *Solanum heterodoxum* released the largest percentage of pollen grains in the first vibration ($46.03\% \pm 5.88$; median \pm se) and *S. grayi* var. *grandiflorum* released the smallest ($0.58\% \pm 0.13$; Table 1). For most species, the amount of pollen released in the first vibration represented more than half of the pollen that was released during the 30 vibrations (Table 2).

For two of the three clades, the dispensing rates were higher in small-flowered taxa than large-flowered taxa, indicating differences in the shapes of the curves. Specifically, the dispensing rates for small-flowered taxa were higher than those of large flower types for the SR-SF clade ($W = 3$, $p = 0.005$, $p_{\text{adjusted}} = 0.01$) and marginally significant for the SC-SH clade ($W = 24$, $p = 0.05$, $p_{\text{adjusted}} = 0.10$), but not for the SGN-SGG clade ($W = 48$, $p = 0.91$, $p_{\text{adjusted}} = 0.91$; Figs. 3 & 4; Table 2). The fast dispensing rates in small-flowered taxa show that these taxa required fewer vibrations to release all the available pollen than large-flowered taxa.

None of the six taxa released all their pollen during 30 vibrations, despite no pollen being released after 30 vibrations. The total amount of pollen released varied strongly between the species of each phylogenetically independent contrast, with large-flowered taxa releasing proportionally fewer pollen grains in 30 vibrations than their small-flowered sister taxon (SC-SH: $W = 2$, $p < 0.001$, $p_{\text{adjusted}} < 0.001$; SR-SF: $W = 48$, $p = 0.002$, $p_{\text{adjusted}} = 0.005$; SGN-SGG: $W = 88$, $p = 0.002$, $p_{\text{adjusted}} = 0.005$; Fig. 4; Table 1). We also observed differences between clades, where the largest proportion of pollen was released by the SC-SH clade and the smallest proportion was released by the SGG-SGN clade.

Effect of vibration properties on pollen dispensing schedules-

The application of different peak vibration velocities resulted in different pollen dispensing schedules. Generally, lower vibration velocities resulted in slower pollen release and less total pollen released over 30 vibrations.

We tested whether the percentage of pollen released in the first vibration varied with vibration velocity, and we found effects of vibration velocity for both the large-flowered *S. citrullifolium* ($F_{2,27} = 11.44$, $p < 0.001$) and the small-flowered *S. heterodoxum* ($F_{2,25} = 21.86$, $p < 0.001$) (Figs. 5 & 6). Tukey posthoc tests showed that for *S. citrullifolium*, a velocity of 80 mm/s released more pollen in the first vibration than both lower velocity vibrations ($SC_{40\text{mm/s}}: p = 0.002$; $SC_{20\text{mm/s}}: p < 0.001$). For each sequential lower velocity vibration, we observed a more than four times decrease in the percentage pollen released (Table 1). Similarly, a velocity of 80 mm/s released more pollen in *S. heterodoxum* plants than both lower velocity vibrations ($SH_{40\text{mm/s}}: p < 0.001$; $SH_{20\text{mm/s}}: p < 0.001$), and we observed a nine-fold decrease in percentage pollen release between velocities of 80 mm/s and 40 mm/s. No differences in pollen released in the first vibration were present between velocities of 40 mm/s and 20 mm/s for either species ($SC: p = 0.85$; $SH: p = 0.76$).

Further, we found differences in the pollen dispensing rates when different vibration velocities were applied. These differences were observed both in *S. citrullifolium* ($F_{2,27} = 10.64$, $p < 0.001$) and in *S. heterodoxum* ($F_{2,25} = 11.50$, $p < 0.001$) (Fig. 6). For *S. citrullifolium*, a velocity of 80 mm/s released pollen quicker than velocities of 40 mm/s ($p = 0.001$) and 20 mm/s ($p < 0.001$), which shows that more vibrations are required to release the available pollen grains when vibration velocities are lower. We observed a three-fold decrease in dispensing rate with a decrease in vibration velocity. Similarly, a velocity of 80 mm/s released pollen quicker in *S. heterodoxum* than velocities of 40 mm/s ($p = 0.02$) and 20 mm/s ($p < 0.001$). However, no differences in pollen dispensing rates were detected between velocities of 40 mm/s and 20 mm/s ($SC: p = 0.91$; $SH: p = 0.45$).

In addition to changes in the shape of the pollen dispensing curves, differences in vibration velocity also influenced the total amount of pollen grains that were ejected, both for *S. citrullifolium* ($F_{2,27} = 4.906$, $p = 0.01$, Figs. 5 & 6) and for *S. heterodoxum* ($F_{2,25} = 25.67$, $p < 0.001$, Figs. 5 & 6). For *S. citrullifolium*, Tukey posthoc tests showed a significant decrease in the total amount of pollen released between 80 and 20 mm/s ($p = 0.01$), but not between 80 and 40 mm/s ($p = 0.26$) nor between 40 and 20 mm/s ($p = 0.28$). Similarly, Tukey posthoc tests showed a significant decrease in the total amount of pollen released for *S. heterodoxum* between 80 and 40 mm/s ($p < 0.001$) and between 80 and 20 mm/s ($p < 0.001$), but not between 40 and 20 mm/s ($p = 0.41$).

Association between pollen dispensing schedules and anther traits-

We tested whether anther traits (i.e., anther wall area and anther pore size) of the feeding and pollinating anthers relate to pollen dispensing, as hypothesized by Buchmann and Hurley (1978). The amount of pollen released in the first vibration was negatively associated with the pollinating anther wall area ($z = -2.232$, $p = 0.03$, Table 2), showing that flowers with larger pollinating anthers release less pollen in the first vibration than those with smaller pollinating anthers. Thus, for each 1 mm^2 increase in pollinating anther area, the log count of pollen released in the first vibration decreases by 0.075 (= 7.8% decrease in pollen grains released). Similarly, pollen dispensing rates were negatively associated with the pollinating anther wall area ($z = -1.952$, $p = 0.05$, Table 2), showing that flowers with larger pollinating anthers release pollen more slowly than flowers with smaller anthers. Thus, with each 1 mm^2 increase in pollinating anther area, the dispensing rate was 10.2% lower. We found no effect of anther pore size in either analysis (Table 2).

DISCUSSION

Our study is the first to systematically investigate the effects of anther morphology and vibration properties on pollen dispensing schedules in buzz-pollinated plants. When applying bee-like vibrations directly to anthers, we found consistent differences in pollen release rates between anther types, where the large anther type released pollen more gradually than the small anther type. Higher vibration velocities resulted in more pollen released in the first vibration and faster pollen release rates, irrespective of the anther type. We thus show that both anther morphology and bee vibrations are associated with pollen release schedules, and likely pollen export, in buzz-pollinated plants. Additionally, we found that larger pollinating anther areas were associated with less pollen released in the first vibration and a slower dispensing rate, showing the potential for relating individual anther traits to pollen release in poricidal taxa.

Pollen dispensing schedules in buzz-pollinated taxa-

Many plant species stagger the pollen release of individual flowers across hours or days (Buchmann et al., 1977; Harder and Barclay, 1994; Sargent, 2003; Castellanos et al., 2006b; Li et al., 2014; Dellinger, Pöllabauer, et al., 2019), and here we show that flowers can also limit pollen release across shorter timeframes (i.e., seconds and minutes). For all six taxa, pollen was released across multiple vibrations, with a smaller amount of pollen released in each successive vibration. This suggests that multiple visits or extended visits by vibrating pollinators are required to extract all of the pollen available for release (see Larson and Barrett, 1999), and that bees would receive the

largest pollen rewards in the first vibration. Most flowers required between three and ten vibrations to release all available pollen grains, which translates to 6 to 20 seconds of buzzing. Our results align with the field observations made by Bowers (1975) which showed that bees tend to spend more time (i.e., 3 – 15 seconds) on newly opened *S. rostratum* flowers and less time on previously visited flowers, presumably matching their visitation lengths with pollen availability.

In line with work on non-poricidal taxa, we also found that pollen release is staggered over longer timeframes. Four of our six taxa released only a small percentage of their total pollen across the thirty vibrations we applied (<20%, median, Fig. 3), even though no pollen was released during the last few vibrations of each trial (see Fig. 2). Because this secondary pollen dosing mechanism does not seem to result from anther morphology, it is likely that pollen maturation or drying of pollenkitt is staggered in these plants, as is seen in other buzz-pollinated taxa (Buchmann et al., 1977; Corbet et al., 1988; King and Ferguson, 1994; King and Buchmann, 1996). Staggering pollen maturation can also allow dynamic adjustment of pollen release schedules to pollinator visitation rates. For instance, if a flower that staggers pollen maturation receives its first visit on the second day of anthesis (e.g., under low visitation rates), then a larger quantity of pollen will be available for extraction than a flower which is visited on the first day (Harder and Barclay 1994). This dynamic adjustment of pollen release to pollinator visitation rates is predicted by theoretical models (Harder and Wilson 1994) and has been shown to occur in other poricidal taxa (Harder and Barclay, 1994; Dellinger, Pöllabauer, et al., 2019).

Shifts in pollen dispensing schedules between flower types-

Theoretical models predict that pollen release schedules should be optimized to pollinator grooming behaviour and pollinator visitation rates (Harder and Thomson, 1989; Harder and Wilson, 1994; LeBuhn and Holsinger, 1998), and empirical work has shown support for these models (Sargent, 2003; Castellanos et al., 2006; Li et al., 2014). A notable study by Castellanos et al. (2006) showed that parallel shifts in *Penstemon* between bee and hummingbird pollination are associated with shifts in anther morphology and pollen dispensing schedules. Similarly, we show that closely-related species in *Solanum* sect. *Androceras*, that have undergone parallel shifts in anther morphology (Vallejo-Marín et al., 2014), have also undergone parallel shifts in their pollen dispensing schedules.

There are at least three non-mutually exclusive hypotheses that could explain the *transition* in dispensing strategy we observed here from slow dispensing in large-flowered taxa to quicker dispensing in small-flowered species: (i) adaptation to a shift in higher selfing rates, (ii) adaptation to a shift in pollinator environment (i.e., lower visitation rate and higher pollen transfer efficiency), and (iii) non-adaptive by-product of the evolution of smaller anthers, which we discuss in turn. (i) *Shift to*

selfing in small flowers. The rapid release of pollen in highly selfing taxa would be expected in small-flowered taxa if selfing is facilitated by pollinators, and thus a single visit by a buzz-pollinating bee can maximise fitness. Moreover, higher rates of pollen release may also be favourable with autonomous selfing if other sources of disturbance to flowers (e.g., induced by wind or non-buzzing floral visitors) might allow pollen release without the assistance of vibrating bees. Although previous work shows that the small-flowered taxa in *Solanum* sect. *Androceras* exhibit traits that correspond to a self-pollination syndrome (Vallejo-Marín et al., 2014; Rubini-Pisano et al., in prep), we currently lack field-estimates of selfing rates of the small-flowered species. Hence this hypothesis remains to be tested further. (ii) *Shift to pollination environments with lower visitation and/or higher pollen transfer efficiency*. In principle, if small-flowered taxa are visited less frequently or visited by pollinators that groom less and efficiently transfer pollen to conspecifics, quicker dispensing strategies could be adaptive. Apart from *S. rostratum*, little is known about the pollination ecology of Section *Androceras*. Whalen (1978) suggested that the transition to small flowers in *Solanum grayii* var. *grayii* was associated with a shift to visitation by smaller bees compared to the large-flowered *S. grayii* var. *grandiflorum*, but we do not know of any detailed characterisations of their pollination ecology. In the large-flowered species *S. rostratum*, both large (e.g. *Xylocopa*) and small bees (e.g., *Lasioglossum*) visit their flowers (Solis-Montero et al. 2015), although larger bees are more likely to contact the sexual organs during visitation (Solis-Montero and Vallejo-Marín 2017). In general, it is unknown to what extent pollinators sort themselves by size across these plant species, and whether visitation rate or pollen-grooming efficiency consistently varies with bee size. Testing the hypothesis that the shift in pollen dispensing is associated with changes in pollination environment (whether associated with smaller pollinators or not) requires additional field observations, particularly among the small-flowered species. (iii) *Non-adaptive by-product of the evolution of smaller flowers*. Changes in dispensing rates in small-flowered taxa could result in the absence of selection on pollen dispensing schedules. We found that smaller anther wall areas are associated with faster dispensing rates. If selection favours the evolution of small flowers for any reason, then smaller flowers could indirectly result in higher pollen dispensing rates simply due to a correlated reduction in anther size. Although we show that pollen dispensing schedules vary consistently between these flower types, field observations and experiments are required to determine the extent to which these three hypotheses could explain differences in pollen dispensing schedules in these species.

The influence of vibration velocity on pollen dispensing schedules-

For a variety of buzz-pollinated taxa, the amount of pollen released in a single vibration increases with vibration velocity when artificial vibrations are applied (Harder and Barclay, 1994; King and Buchmann, 1996; De Luca et al. 2013) as predicted by Buchmann and Hurley's (1978) model. Here,

we show for the first time that vibration velocity also influences the amount of pollen released in successive vibrations. Low velocity vibrations resulted in slower pollen dispensing rates, with less pollen dispensed during 30 vibrations. Accordingly, bees that produce low velocity vibrations are unlikely to extract large pollen quantities. These bees would either need to visit multiple flowers or they would potentially be discouraged from visiting these plants (Harder, 1990b; Nicholls and Hempel de Ibarra, 2017). Poricidal anthers could thus act as filter to insect taxa that cannot produce the necessary vibrations (De Luca and Vallejo-Marín, 2013; Sun and Rychtář, 2015; van der Kooi et al., in press), and restrict access to pollen rewards in a similar way in which long nectar tubes exclude insects with short proboscides from accessing nectar rewards (Newman et al., 2014; Santamaría and Rodríguez-Gironés, 2015; Zung et al., 2015). This vibration filter might be particularly effective in discouraging visitation from small bees that produce lower velocity vibrations (De Luca et al., 2013, 2019) and do not make contact with reproductive organs (Solís-Montero and Vallejo-Marín, 2017). However, some bee taxa might be able to adjust their vibration velocities or duration (Harder and Barclay, 1994; Morgan et al., 2016; Russell et al., 2016), resulting in increased pollen extraction at a higher energy cost to the insect. Field observations of the large flowered *S. rostratum* have shown that small buzzing bees frequently visit flowers (Solís-Montero et al., 2015), but larger taxa that produce higher velocity vibrations (De Luca et al., 2019), such as *Bombus* and *Xylocopa*, are common visitors (Whalen, 1978), as well as efficient pollinators (Solís-Montero and Vallejo-Marín, 2017).

Although bees that produce high velocity vibrations are the most effective at extracting pollen, attracting such visitors might not always be the best strategy for plants. Optimal dispensing schedules are contingent on pollinator grooming behaviours (Harder and Thomson, 1989), and if bees groom large amounts of pollen per visit, then slower dispensing (as induced by lower velocity vibrations) should theoretically result in higher plant fitness. Additionally, optimal dispensing schedules are dependent on pollinator visitation rates, and these are likely to be dependent on bee and plant community composition. Sargent (2003) showed that temporal changes in pollinator community composition and visitation rates were associated with temporal within-species changes in pollen dispensing rates. Thus, if pollinator visitation rates are low, quick dispensing will be favoured, even if bees collect large amounts of pollen per visit. Optimal dispensing schedules are thus expected to be adapted to the ecological community context, as well as the behaviour of bees.

Anther traits and pollen dispensing schedules-

Our results clearly show that pollen dispensing schedules are associated with both anther type and vibration properties. However, connecting pollen release schedule variation to specific anther traits is much more challenging. We find that larger anther areas are associated with less pollen released

in the first vibration (Table 2a) and reduced pollen release rates (Table 2b). These effects are statistically significant for pollinating anthers, but not for feeding anthers (Table 2). This suggests that other aspects of the morphology and material properties of anthers that are not captured by the model, such as anther tapering, anther inner surface structure or pollen properties, might be important in pollen release. It further suggests that the ability of the current biophysical model to predict pollen release might be more accurate for some anther morphologies than others, and this warrants further investigation.

Our results contrast with the expectation generated by the Buchmann and Hurley (1978) model that large anther locule areas should be associated with higher dispensing rates. However, their model also predicts a negative association between anther locule volume and pollen dispensing rates. Because anther wall area and anther locule volume are linked, we are potentially detecting the effects of locule volume rather than locule wall area. Quantifying the internal volume of anther locules is difficult but possible using techniques such as X-ray micro-computer tomography scanning (Dellinger, Artuso, et al., 2019), and our work suggests that this is likely an important variable to measure. The lack of a statistically significant association between pore size and pollen release parameters is intriguing, but perhaps not unexpected given smaller variation in pore sizes than anther areas (see Fig. 1), as well as the conflicting effects of pore area on pollen release in the theoretical model of Buchmann and Hurley (1978).

CONCLUSIONS AND FUTURE DIRECTIONS

Our focal taxa stagger pollen release across multiple vibrations, and this is likely common in other poricidal species (Corbet et al., 1988; Harder, 1990; Harder and Barclay, 1994; Dellinger, Pöllabauer, et al., 2019). This gradual release of pollen will influence pollen export dynamics of plants and the amount of reward that bees receive per visit. We show that high-velocity vibrations result in more pollen released per vibration, and thus bees that can produce such vibrations will receive higher reward quantities. The observed pollen dispensing schedules likely reflect an optimization that maximises pollen export whilst providing sufficient rewards to pollinators.

Our results highlight the need for more empirical studies of pollen dispensing schedules in buzz-pollinated plants, as well as for developing biophysical models of buzz-pollination that incorporate additional aspects of the morphology, geometry and material properties of flowers. The vibrations that the anthers experience depend both on the characteristics of bee vibrations (Switzer et al., 2019; Pritchard and Vallejo-Marín, 2020) and on the properties of the floral structures (Arroyo-Correa et al., 2019). For example, the transmission of vibrations through the flower can alter the vibration that the anther experiences, e.g., by dampening the vibration velocity (King, 1993,

which can vary between closely-related taxa (Arroyo-Correa et al., 2019). In contrast, if the bee vibrates the anther at its natural frequency (Nunes et al., 2020), resonance could amplify anther velocity and result in higher pollen removal (King and Buchmann, 1996). Joint modelling and experimental approaches to buzz pollination have the potential to help us understand the biomechanics and function of a fascinating biological interaction involving thousands of plant and bee species.

ACKNOWLEDGMENTS

We thank the members of the Vallejo-Marín lab for fruitful conversations on buzz-pollination and help with plant maintenance, with particular thanks to Carlos Pereira Nunes. We thank Ian Washbourne and George MacLeod for assistance with the use of the particle counter and SEM respectively, and Boris Igic and Lislie Solís-Montero for collaborating with the fieldwork to collect seed material. We thank the Associate Editor and two anonymous reviewers for their constructive comments. The project was made possible by the Royal Society of London and the Newton Fund through a Newton International Fellowship to JEK (NIF/R1/181685), by a Scottish Plant Health License (PH/38/2018-2020), and a research grant from The Leverhulme Trust (RPG-2018-235) to MVM.

AUTHOR CONTRIBUTIONS

Investigation (conducting experiments and data collection): JEK. Conceptualisation, visualisation, formal analysis, writing and funding acquisition: JEK and MVM.

DATA AVAILABILITY

The data associated with this paper is available at the University of Stirling's DataSTORRE repository.

SUPPORTING INFORMATION

Additional Supporting Information may be found online in the supporting information section at the end of the article.

Appendix S1. Plant material of *Solanum* section *Androceras* used in this study.

596 Appendix S2. Artificial vibrations applied to anthers. (a) Each stimulus consisted of five short
597 vibration pulses of 0.2 s long, with 0.2 s of silence between pulses. (b) The beginning of each 0.2 s
598 pulse consisted of a short fade-in, which is similar to what bees produce and it ensures that the
599 wave is transmitted in the expected manner.

600 Appendix S3. The custom-made vibration transducer system. Vibrations were transferred from a
601 laptop to (1) a speaker. From there, vibrations were transferred to (2) a metal rod that was attached
602 in the speaker with glue. Vibrations then travelled from the rod through (3) a metal clip that was
603 tightly attached to the metal rod and fixed using glue. From there, vibrations were transferred to (4)
604 forceps, and then to (5) anthers. The anthers were clasped approximately where a bee would attach.
605 Please note that in our experiments, we used storkbill short blunt forceps (D4045, Watkins &
606 Doncaster, UK) and not the long-pronged forceps depicted here.

607 Appendix S4. For each anther, the length (solid line) and breadth (dashed line) was measured. For
608 each anther type within a flower the pore area was measure for one feeding and one pollinating
609 anther. The photo shows a SEM image of a *Solanum fructu-tecto* feeding anther. The scale bar
610 represents 200 μm .

611

612 LITERATURE CITED

- 613 Arceo-Gómez, G., M. L. Martínez, V. Parra-Tabla, and J. G. García-Franco. 2011. Anther and stigma
614 morphology in mirror-image flowers of *Chamaecrista chamaecristoides* (Fabaceae):
615 Implications for buzz pollination. *Plant Biology* 13: 19–24.
- 616 Arroyo-Correa, B., C. Beattie, and M. Vallejo-Marín. 2019. Bee and floral traits affect the
617 characteristics of the vibrations experienced by flowers during buzz pollination. *Journal of*
618 *Experimental Biology* 222: jeb198176.
- 619 Bowers, K.A.W. 1975. The pollination ecology of *Solanum rostratum* (Solanaceae). *American Journal*
620 *of Botany* 62: 633–638.
- 621 Buchmann, S. L., C. E. Jones, and L.J. Colin. 1977. Vibratile pollination of *Solanum douglasii* and *S.*
622 *xanti* (Solanaceae) in southern California. *The Wasmann Journal of Biology* 35: 1–25.
- 623 Buchmann, S. L. 1983. Buzz pollination in angiosperms. *Handbook of Experimental Pollination*
624 *Biology*. In: Jones CE, Little RJ, eds. *Handbook of experimental pollination biology*. New York,
625 NY: Scientific and Academic Editions, 73–113.
- 626 Buchmann, S. L., and J. P. Hurley. 1978. A biophysical model for buzz pollination in angiosperms.
627 *Journal of Theoretical Biology* 72: 639–657.
- 628 Cardinal, S., S. L. Buchmann, and A. L. Russell. 2018. The evolution of floral sonication: a pollen
629 foraging behavior used by bees (Anthophila). 590–600.
- 630 Castellanos, M. C., P. Wilson, S. J. Keller, A. D. Wolfe, and J. D. Thomson. 2006. Anther evolution:
631 pollen presentation strategies when pollinators differ. *The American Naturalist* 167: 288–296.
- 632 Corbet, S. A., H. Chapman, and N. Saville. 1988. Vibratory pollen collection and flower form: bumble-
633 bees on *Actinidia*, *Symphytum*, *Borago* and *Polygonatum*. *Functional Ecology* 2: 147-155.
- 634 Corbet, S. A., and S. Q. Huang. 2014. Buzz pollination in eight bumblebee-pollinated *Pedicularis*
635 species: Does it involve vibration-induced triboelectric charging of pollen grains? *Annals of*
636 *Botany* 114: 1665–1674.
- 637 Dellinger, A. S., S. Artuso, S. Pamperl, F. A. Michelangeli, D. S. Penneys, D. M. Fernández-Fernández,
638 M. Alvear, et al. 2019. Modularity increases rate of floral evolution and adaptive success for
639 functionally specialized pollination systems. *Communications Biology* 2: 453.
- 640 Dellinger, A. S., M. Chartier, D. Fernández-Fernández, D. S. Penneys, M. Alvear, F. Almeda, F. A.
641 Michelangeli, et al. 2019. Beyond buzz-pollination—departures from an adaptive plateau lead to

new pollination syndromes. *New Phytologist* 221: 1136–1149.

Dellinger, A. S., L. Pöllabauer, M. Loreti, J. Czurda, and J. Schönenberger. 2019. Testing functional hypotheses on poricidal anther dehiscence and heteranthery in buzz-pollinated flowers. *Acta ZooBot Austria* 156: 197–214.

Dulberger, R., M. B. Smith, and K. S. Bawa. 1994. The stigmatic orifice in *Cassia*, *Senna*, and *Chamaecrista* (Caesalpiniaceae): Morphological variation, function during pollination, and possible adaptive significance. *American Journal of Botany* 81: 1390–1396.

Faegri, K. 1986. The solanoid flower. *Transactions of the Botanical Society of Edinburgh* 45: 51–59.

Harder, L. D. 1990. Behavioral responses by bumble bees to variation in pollen availability. *Oecologia* 85: 41–47.

Harder, L. D., and R. M. R. Barclay. 1994. The functional significance of poricidal anthers and buzz pollination: controlled pollen removal from *Dodecatheon*. *Functional Ecology* 8: 509–517.

Harder, L. D., and S. D. Johnson. 2009. Darwin’s beautiful contrivances: evolutionary and functional evidence. *New Phytologist* 183: 530–545.

Harder, L. D., and J. D. Thomson. 1989. Evolutionary options for maximizing pollen dispersal of animal-pollinated plants. *The American Naturalist* 133: 323–344.

Harder, L. D., and W. G. Wilson. 1994. Floral evolution and male reproductive success: Optimal dispensing schedules for pollen dispersal by animal-pollinated plants. *Evolutionary Ecology* 8: 542–559.

Harris, J. A. 1905. The dehiscence of anthers by apical pores. *Missouri Botanical Garden Report*: 167–257.

Holsinger, K. E., and J. D. Thomson. 1994. Pollen discounting in *Erythronium grandiflorum*: mass-action estimates from pollen transfer dynamics. *The American Naturalist* 144: 799–812.

King, M. J. 1993. Buzz foraging mechanism of bumble bees. *Journal of Apicultural Research* 32: 41–49.

King, M. J., and S. L. Buchmann. 2003. Floral sonication by bees: Mesosomal vibration by *Bombus* and *Xylocopa*, but not *Apis* (Hymenoptera: Apidae), ejects pollen from poricidal anthers. *Journal of Kansas Entomological Society* 76: 295–305.

King, M. J., and S. L. Buchmann. 1996. Sonication dispensing of pollen from *Solanum laciniatum*

671 flowers. *Functional Ecology* 10: 449–456.

672 King, M. J., S. L. Buchmann, and H. Spangler. 1996. Activity of asynchronous flight muscle from two
673 bee families during sonication (buzzing). *Journal of Experimental Biology* 199: 2317–2321.

674 King, M. J., and A. M. Ferguson. 1994. Vibratory Collection of *Actinidia deliciosa* (Kiwifruit) Pollen.
675 *Annals of Botany* 74: 479–482.

676 Knapp, S. 2002. Floral diversity and evolution in the Solanaceae. In: Developmental genetics and
677 plant evolution, 267–297.

678 Larson, B. M. H., and S. C. H. Barrett. 1999. The pollination ecology of buzz-pollinated *Rhexia*
679 *virginica* (Melastomataceae). *American Journal of Botany* 86: 502–511.

680 LeBuhn, G., and K. Holsinger. 1998. A sensitivity analysis of pollen-dispersing schedules. *Evolutionary*
681 *Ecology* 12: 111–121.

682 Li, X. X., H. Wang, R. W. Gituru, Y. H. Guo, and C. F. Yang. 2014. Pollen packaging and dispensing:
683 Adaption of patterns of anther dehiscence and flowering traits to pollination in three
684 *Epimedium* species. *Plant Biology* 16: 227–233.

685 De Luca, P. A., S. Buchmann, C. Galen, A. C. Mason, and M. Vallejo-Marín. 2019. Does body size
686 predict the buzz-pollination frequencies used by bees? *Ecology and Evolution* 9: 4875–4887.

687 De Luca, P. A., L. F. Bussière, D. Souto-Vilaros, D. Goulson, A. C. Mason, and M. Vallejo-Marín. 2013.
688 Variability in bumblebee pollination buzzes affects the quantity of pollen released from
689 flowers. *Oecologia* 172: 805–816.

690 De Luca, P. A., and M. Vallejo-Marín. 2013. What’s the ‘buzz’ about? The ecology and evolutionary
691 significance of buzz-pollination. *Current Opinion in Plant Biology* 16: 429–435.

692 Minnaar, C., B. Anderson, M. L. De Jager, and J. D. Karron. 2019. Plant–pollinator interactions along
693 the pathway to paternity. *Annals of Botany* 123: 225–245.

694 Morgan, T., P. Whitehorn, G. C. Lye, and M. Vallejo-Marín. 2016. Floral sonication is an innate
695 behaviour in bumblebees that can be fine-tuned with experience in manipulating flowers.
696 *Journal of Insect Behavior* 29: 233–241.

697 Newman, E., J. Manning, and B. Anderson. 2014. Matching floral and pollinator traits through guild
698 convergence and pollinator ecotype formation. *Annals of Botany* 113: 373–384.

699 Nicholls, E., and N. Hempel de Ibarra. 2017. Assessment of pollen rewards by foraging bees.

700 *Functional Ecology* 31: 76–87.

701 Nunes, C.E.P., L. Nevard, F. Montealegre-Zapata, and M. Vallejo-Marin. 2020. Are flowers tuned to
702 buzzing pollinators? Variation in the natural frequency of stamens with different morphologies
703 and its relationship to bee vibrations. *bioRxiv*. doi: <https://doi.org/10.1101/2020.05.19.104422>.

704 Ollerton, J., R. Winfree, and S. Tarrant. 2011. How many flowering plants are pollinated by animals?
705 *Oikos* 120: 321–326.

706 Pritchard, D.J., and M. Vallejo-Marín. 2020. Floral vibrations by buzz-pollinating bees achieve higher
707 frequency , velocity and acceleration than flight and defence vibrations. *Journal of*
708 *Experimental Biology* 223:11.

709 R Core Team. 2019. R: A language and environment for statistical computing. R Core Team. Vienna,
710 Austria. <http://www.R-project.org/>

711 Rosi-Denadai, C. A., P. C. S. Araújo, L. A. de O. Campos, L. Cosme, and R. N. C. Guedes. 2018. Buzz-
712 pollination in Neotropical bees: genus-dependent frequencies and lack of optimal frequency for
713 pollen release. *Insect Science* 27: 133–142.

714 Rubini Pisano, A., M. Vallejo-Marín, S. Benitez-Vieyra, and J. Fornoni. In review. From large to small
715 flowers in *Solanum* (Section *Androceras*): a multivariate perspective.

716 Russell, A. L., A. S. Leonard, H. D. Gillette, and D. R. Papaj. 2016. Concealed floral rewards and the
717 role of experience in floral sonication by bees. *Animal Behaviour* 120: 83–91.

718 Santamaría, L., and M. a. Rodríguez-Gironés. 2015. Are flowers red in teeth and claw? Exploitation
719 barriers and the antagonist nature of mutualisms. *Evolutionary Ecology* 29: 311–322.

720 Sargent, R. D. 2003. Seasonal changes in pollen-packaging schedules in the protandrous plant
721 *Chamerion angustifolium*. *Population Ecology* 135: 221–226.

722 Särkinen, T., L. Bohs, R. G. Olmstead, and S. Knapp. 2013. A phylogenetic framework for evolutionary
723 study of the nightshades (Solanaceae): A dated 1000-tip tree. *BMC Evolutionary Biology* 13.

724 Schlindwein, C., D. Wittmann, C. F. Martins, a. Hamm, J. a. Siqueira, D. Schiffler, and I. C. MacHado.
725 2005. Pollination of *Campanula rapunculus* L. (Campanulaceae): How much pollen flows into
726 pollination and into reproduction of oligolectic pollinators? *Plant Systematics and Evolution*
727 250: 147–156.

728 Schneider, C. A., W. S. Rasband, and K. W. Eliceiri. 2012. NIH Image to ImageJ: 25 years of image
729 analysis. *Nature Methods* 9: 671–675.

730 Solis-Montero, L., C. Vergara, and M. Vallejo-Marín. 2015. High incidence of pollen theft in natural
731 populations of a buzz-pollinated plant. *Arthropod-Plant Interactions* 9: 599-611.

732 Solis-Montero, L., and M. Vallejo-Marín. 2017. Does the morphological fit between flowers and
733 pollinators affect pollen deposition? An experimental test in a buzz-pollinated species with
734 anther dimorphism. *Ecology and Evolution* 7: 2706-2715.

735 Stern, S. R., T. Weese, and L. A. Bohs. 2010. Phylogenetic relationships in *Solanum* section
736 *Androceras* (Solanaceae). *Systematic Botany* 35: 885–893.

737 Sun, S., and J. Rychtář. 2015. The screening game in plant–pollinator interactions. *Evolutionary*
738 *Ecology* 29: 479–487.

739 Switzer, C. M., and S. A. Combes. 2017. Bumblebee sonication behavior changes with plant species
740 and environmental conditions. *Apidologie* 48: 223–233.

741 Switzer, C.M., A. Russell, D. Papaj, S. Combes, and R. Hopkins. 2019. Sonicating bees demonstrate
742 flexible pollen extraction without instrumental learning. *Current Zoology* 65: 425-436.

743 Thomson, J. D. 1986. Pollen transport and deposition by bumble bees in *Erythronium*: influences of
744 floral nectar and bee grooming. *Journal of Ecology* 74: 329–341.

745 Vallejo-Marín, M. 2019. Buzz pollination: studying bee vibrations on flowers. *New Phytologist* 224:
746 1068–1074.

747 Vallejo-Marín, M., J. S. Manson, J. D. Thomson, and S. C. H. Barrett. 2009. Division of labour within
748 flowers: Heteranthery, a floral strategy to reconcile contrasting pollen fates. *Journal of*
749 *Evolutionary Biology* 22: 828–839.

750 Vallejo-Marín, M., E. M. Da Silva, R. D. Sargent, and S. C. H. Barrett. 2010. Trait correlates and
751 functional significance in flowering of heteranthery plants. *New Phytologist* 188(2): 418-425.

752 Vallejo-Marín, M., C. Walker, P. Friston-Reilly, L. Solís-Montero, and B. Igic. 2014. Recurrent
753 modification of floral morphology in heterantherous *Solanum* reveals a parallel shift in
754 reproductive strategy. *Philosophical Transactions of the Royal Society B: Biological Sciences*
755 369: 20130256.

756 van der Kooi, C. J., M. Vallejo-Marín, S.D. Leonhardt. *In Press*. Mutualisms and (a)symmetry in plant-
757 pollinator interactions. *Current Biology*. Whalen, M. D. 1979. Allozyme variation and evolution
758 in *Solanum* section *Androceras*. *American Society of Plant Taxonomists* 4: 203–222.

759 Whalen, M. D. 1978. Reproductive character displacement and floral diversity in *Solanum* section

760 *Androceras*. *Systematic Biology* 3: 77–86.

761 Zung, J. L., J. R. K. Forrest, M. C. Castellanos, and J. D. Thomson. 2015. Bee- to bird-pollination shifts

762 in *Penstemon*: effects of floral-lip removal and corolla constriction on the preferences of free-

763 foraging bumble bees. *Evolutionary Ecology* 29: 341–354.

764

765 TABLES

766 **Table 1.** POLLEN dispensing schedule metrics for six *Solanum* taxa during simulated buzz pollination. In each treatment, flowers were subjected to 30
 767 vibrations. All species were subjected to vibrations with a peak velocity of 80 mm/s and frequency of 300 Hz (which equals an acceleration of 151 m/s² and
 768 a displacement of 42 µm). Two species (*Solanum citrullifolium* and *S. heterodoxum*) were also exposed to two lower velocity vibrations, i.e., 40 mm/s
 769 (acceleration = 75 m/s²; displacement = 21 µm) and 20 mm/s (acceleration = 38m/s²; displacement = 11 um). Median ± standard error. *N* = sample size.

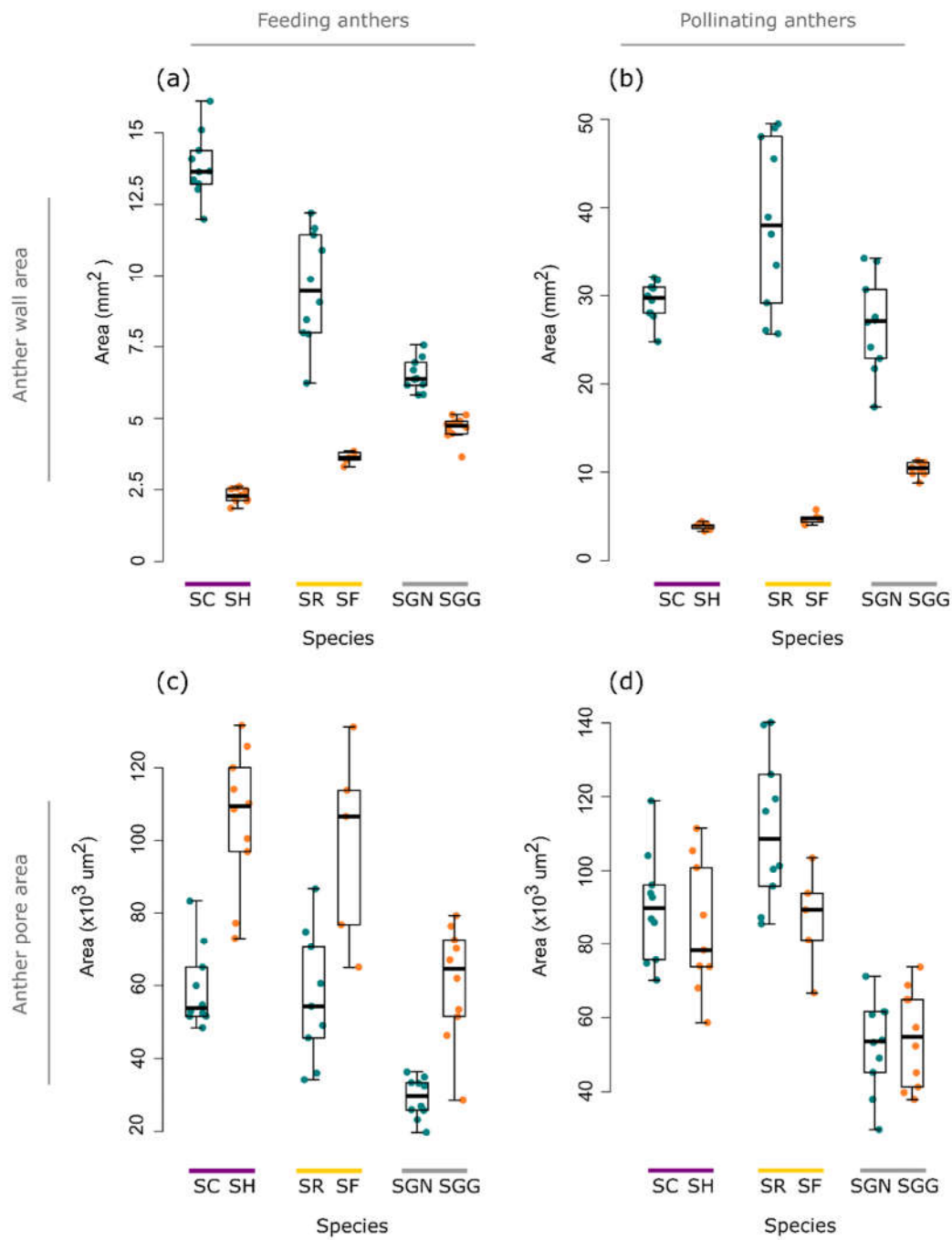
Species	Pollen grains per flower (x10 ³)	Frequency (Hz)	Peak velocity (mm/s)	Percentage pollen released in first vibration	Dispensing rate <i>b</i>	Percentage pollen released in 30 vibrations	<i>N</i>
Series Androceras (SC-SH clade)							
<i>S. citrullifolium</i>	180 ± 12	300	80	9.54 ± 2.62	0.69 ± 0.09	17.50 ± 3.33	10
		300	40	2.16 ± 2.95	0.22 ± 0.12	10.98 ± 2.00	10
		300	20	0.13 ± 0.08	0.05 ± 0.09	4.61 ± 2.08	10
<i>S. heterodoxum</i>	22 ± 2	300	80	46.03 ± 5.88	0.87 ± 0.08	61.55 ± 6.02	10
		300	40	4.81 ± 3.32	0.35 ± 0.09	17.45 ± 4.10	9
		300	20	1.31 ± 1.82	0.08 ± 0.10	7.14 ± 4.78	9
Series Pacificum (SR-SF clade)							
<i>S. rostratum</i>	288 ± 71	300	80	2.52 ± 0.97	0.38 ± 0.06	7.97 ± 1.55	10

<i>S. fructu-tecto</i>	76 ± 8	300	80	21.40 ± 7.33	0.60 ± 0.05	38.47 ± 10.64	5
Series Violaceiflorum							
(SGN-SGG clade)							
<i>S. grayi</i> var.	466 ± 53	300	80	0.58 ± 0.13	0.28 ± 0.08	1.77 ± 0.44	10
<i>grandiflorum</i>							
<i>S. grayi</i> var. <i>grayi</i>	113 ± 11	300	80	1.63 ± 0.55	0.35 ± 0.08	4.75 ± 1.25	10

770

Table 2. ASSOCIATION between pollen dispensing schedules and various anther traits assessed using mixed-effect models. (a) Negative binomial mixed effect model with species identity as random factor. We used the number of pollen grains released in the first vibration as response variable, and tested whether this is associated with the anther wall area and anther pore area of the feeding and pollinating anthers separately. We used the total amount of pollen in a flower as offset in the model. (b) Logistic mixed-effects model with species identity as random factor. We used untransformed pollen dispensing rates (b ; ranging from 0 to 1) as response variable (with high values indicating most pollen is released in few vibrations) and tested whether this was associated with the anther wall area and anther pore area of the feeding and pollinating anthers separately. Significance at $P < 0.05$ is indicated in bold.

(a) Pollen released in first vibration			
Variable	Coefficient	SE	<i>P</i> -value
Intercept	-3.2191	0.8657	
<i>Feeding anther:</i>			
Area (mm ²)	0.0299	0.0319	0.35
Pore size (mm ²)	2.1685	1.7722	0.22
<i>Pollinating anther:</i>			
Area (mm ²)	-0.0751	0.0336	0.03
Pore size (mm ²)	5.4196	4.3688	0.21
(b) Pollen dispensing rate (<i>b</i>)			
Fixed effect	Coefficient	SE	<i>P</i> -value
Intercept	-0.2263	1.2193	
<i>Feeding anther:</i>			
area	0.0471	0.0313	0.13
pore size	0.3294	4.0790	0.94
<i>Pollinating anther:</i>			
area	-0.0973	0.0499	0.05
pore size	8.8027	16.7648	0.60



784

785

786 **Figure 1.** Anther wall (top panel) and anther pore areas (bottom panel) for the feeding (lefthand
787 panel) and pollinating (righthand panel) anthers of three pairs of taxa in *Solanum* section *Androceras*
788 (*Solanaceae*). Anther wall area was calculated following Buchmann and Hurley (1978) as the product
789 of the length and breadth of anthers. Anther pore area was measured from SEM photographs. We

790 show the values of individual anthers, and not the summed values used in the analyses. The six
791 studied taxa belong to three phylogenetic clades indicated by the purple, yellow and grey lines
792 above taxon names. Within each clade, blue dots indicate the large-flowered type and orange dots
793 indicate the small-flowered type. Species names are: SC = *Solanum citrullifolium*; SH = *S.*
794 *heterodoxum*; SR = *rostratum*; SF = *S. fructu-tecto*; SGN = *S. grayi* var. *grandiflorum*; SGG = *S. grayi*
795 var. *grayi*.
796

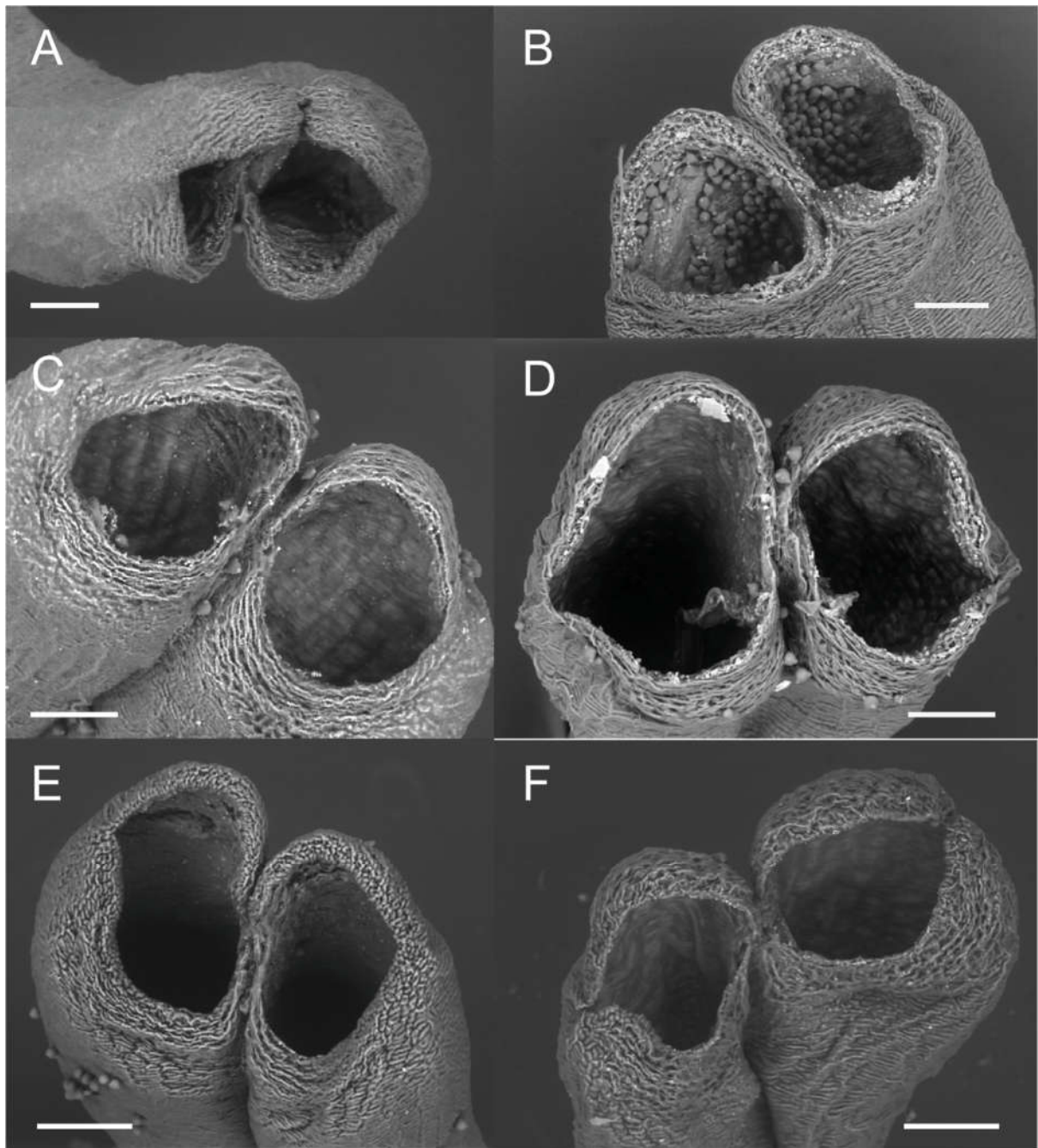
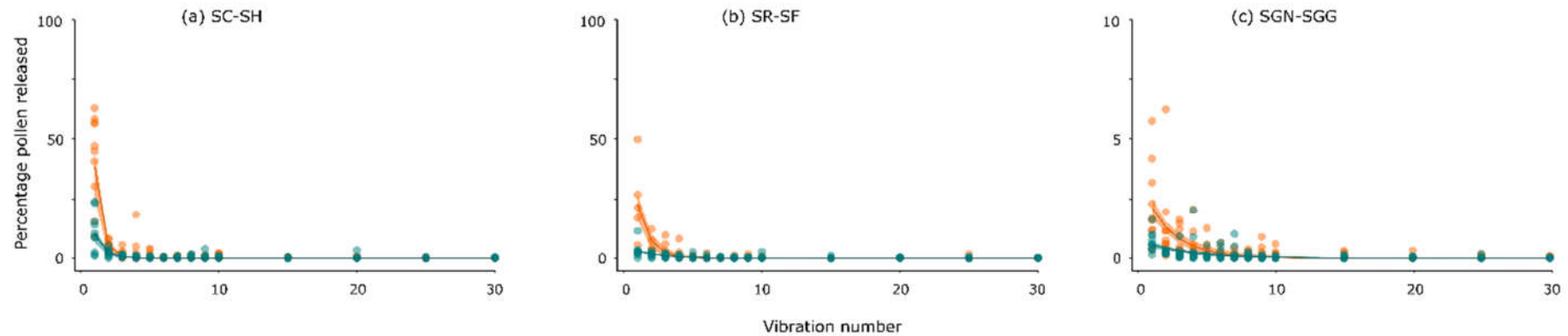


Figure 2. Pores of the pollinating anthers of (A) *Solanum rostratum*, (B) *S. fructu-tecto*, (C) *S. citrullifolium*, (D) *S. heterodoxum*, (E) *S. grayi* var. *grandiflorum*, and (F) *S. grayi* var. *grayi*. The panel on the left represent species of the “large flower” type, and the panel on the right shows species of the “small flower” type.

804



805

806

807 **Figure 3.** Pollen dispensing curves for three pairs of taxa in *Solanum* sect. *Androceras*, belonging to three phylogenetic clades: (a) Series *Violaceiflorum* (b)
 808 Series *Androceras*, and (c) Series *Pacificum*. Each point shows the percentage of pollen released per vibration. Orange curves show the small flower type,
 809 and blue curves show the large flower type. These curves were fitted using *nls* in R and are based on the combined data of all flowers of a species.
 810 Confidence intervals (95%) were fitted using *predictNLS*. Species names as in Figure 1.

811

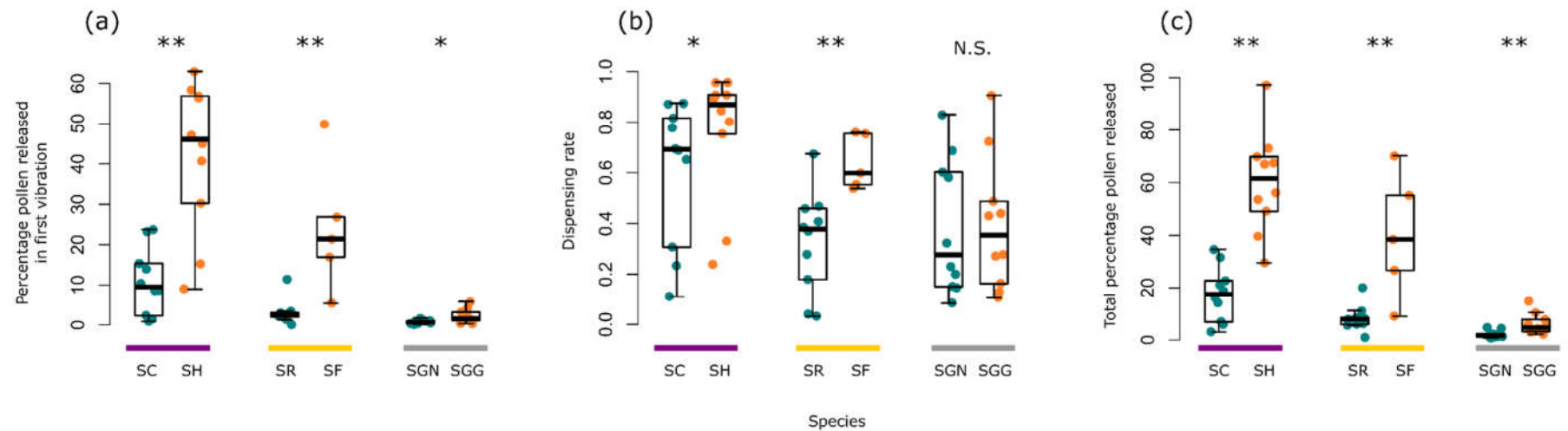


Figure 4. (a) The percentage pollen released in the first vibration is compared between flower types within the three clades, indicated by the purple, yellow and grey lines. For all clades, the small flower type released more pollen in the first vibration than the large flower type. (b) The dispensing rate is compared between flower types within the three clades. For two clades, the small flower type released pollen faster than the large flower type. (c) The total percentage pollen released across 30 vibrations is compared between flower types within clades. For all clades, the small flower type released more of its pollen than the large flower type. Orange curves show the small flower type, and blue curves show the large flower type. Species names as in Figure 1. * 0.01 < p < 0.05; ** 0.001 < p < 0.01.

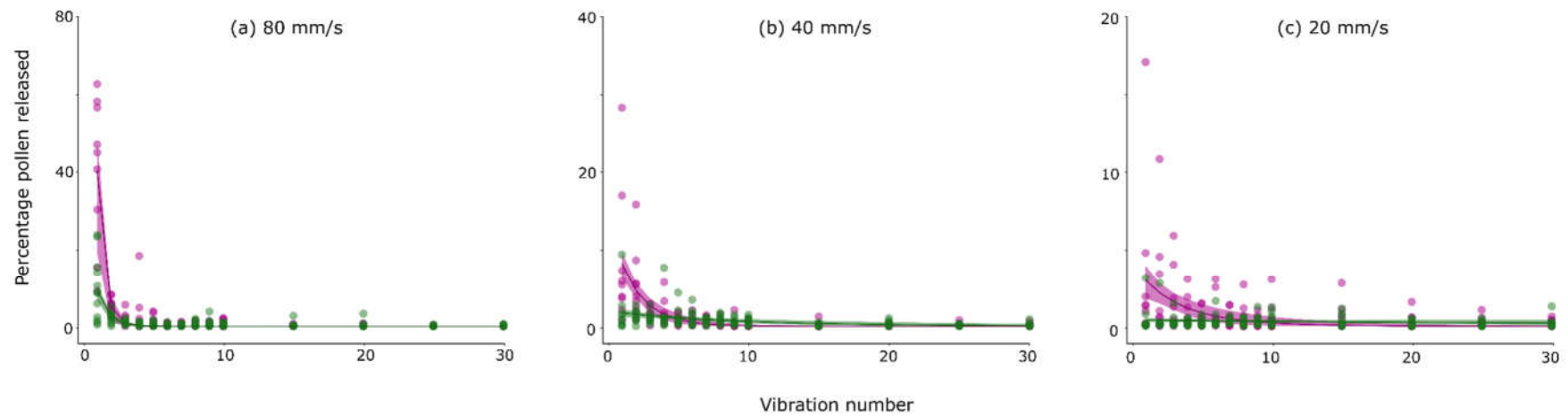


Figure 5. Pollen dispensing curves for *Solanum citrullifolium* (in green; large flower type) and *S. heterodoxum* (in pink; small flower type) when (a) 80 mm/s, (b) 40 mm/s, and (c) 20 mm/s vibration velocities were applied to flowers. Each point shows the percentage of pollen released per vibration. These curves were fitted using *nls* in R and are based on the combined data of all flowers of a species. Confidence intervals (95%) were fitted using *predictNLS*.

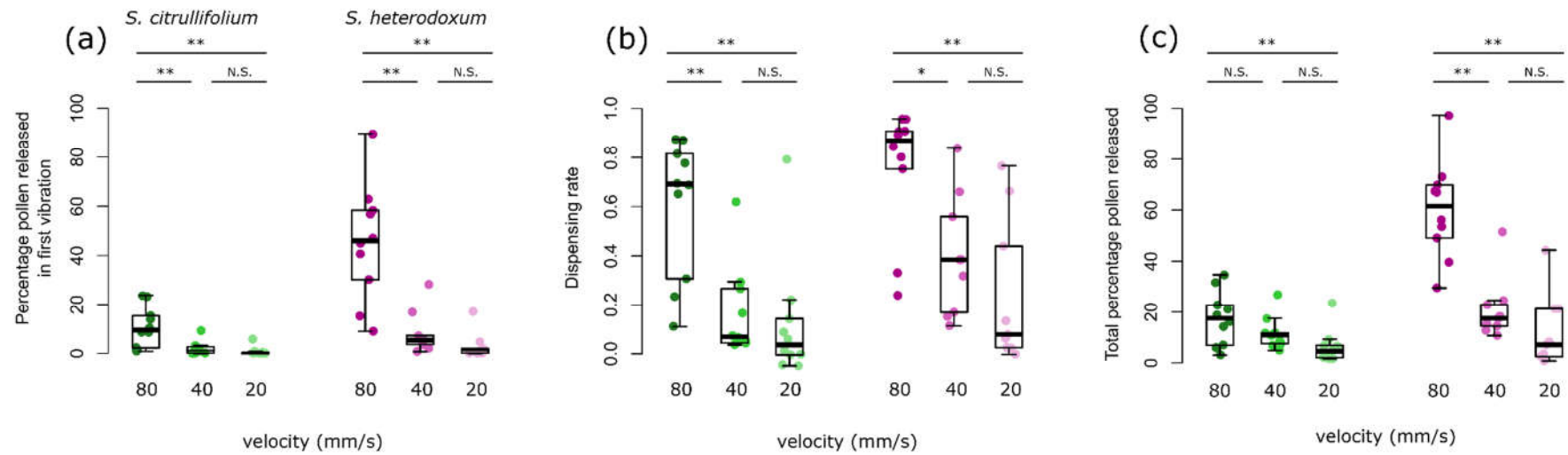


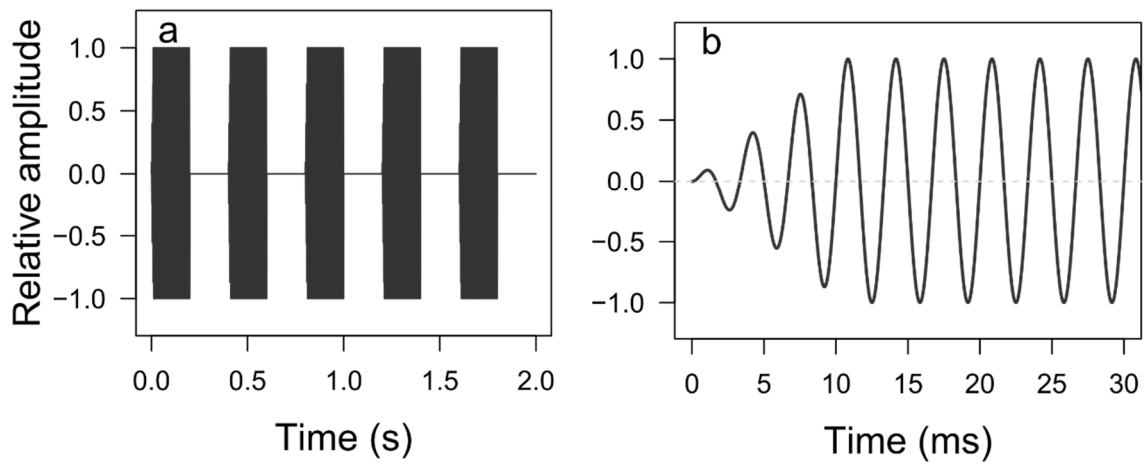
Figure 6. The percentage pollen released in the first vibration (a), the dispensing rate (b), and the total percentage pollen released across 30 vibrations (c) are compared between vibration velocities for *S. citrullifolium* (in green; large flower type) and *S. heterodoxum* (in pink; small flower type). * $0.01 < p < 0.05$; ** $0.001 < p < 0.01$.

832 **Appendix S1.** Plant material of *Solanum* section *Androceras* used in this study.

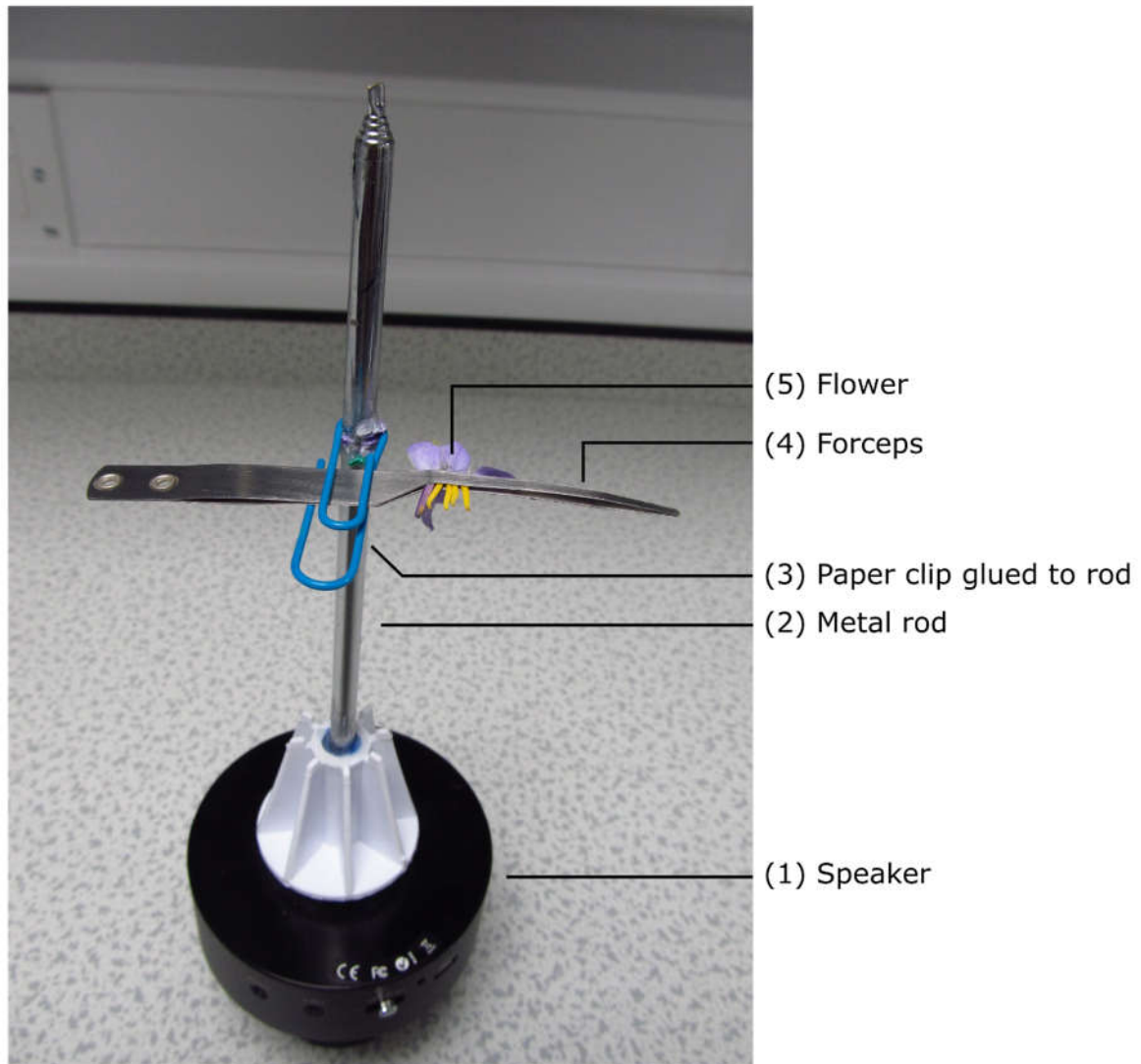
Accession number	Species	Section	Population name	Latitude (N)	Longitude (W)
199-7-3	<i>S. citrullifolium</i>	Violaceiflorum	Nijmegen Collection	-	-
11-PTM-14, 15	<i>S. heterodoxum</i>		Teotihuacán, Estado de México	19.68	98.84
10-s-81, 82, 86	<i>S. rostratum</i>	Androceras	San Miguel de Allende, Querétaro	20.90	100.45
10-AH-9, 24	<i>S. fructu-tecto</i>		Atitalaquia, Hidalgo	20.06	99.21
08-s-78, 79	<i>S. grayi</i> var. <i>grandiflorum</i>	Pacificum	Tejupilco, Estado de México	18.85	100.13
07-s-194b, 195b, 196b	<i>S. grayi</i> var. <i>grayi</i>		Los Álamos, Sonora	27.00	108.93

833

Appendix S2. Artificial vibrations applied to anthers. (a) Each stimulus consisted of five short vibration pulses of 0.2 s long, with 0.2 s of silence between pulses. (b) The beginning of each 0.2 s pulse consisted of a short fade-in, which is similar to what bees produce and it ensures that the wave is transmitted in the expected manner.



Appendix S3. The custom-made vibration transducer system. Vibrations were transferred from a laptop to (1) a speaker. From there, vibrations were transferred to (2) a metal rod that was attached in the speaker with glue. Vibrations then travelled from the rod through (3) a metal clip that was tightly attached to the metal rod and fixed using glue. From there, vibrations were transferred to (4) forceps, and then to (5) anthers. The anthers were clasped approximately where a bee would attach. Please note that in our experiments, we used storkbill short blunt forceps (D4045, Watkins & Doncaster, UK) and not the long-pronged forceps depicted here.



Appendix S4. For each anther, the length (solid line) and breadth (dashed line) was measured. For each anther type within a flower the pore area was measure for one feeding and one pollinating anther. The photo shows a SEM image of a *Solanum fructu-tecto* feeding anther. The scale bar represents 200 μm .

